STAT

COPY 2 OF 5

Project 9043

Final Report

STATOTHR

Approved For Release 2003/08/04 : CIA-RDP78B04747A003100010061-0

Table of Contents

Approved For Release 2003/08/04 : CIA-RDP78B04747A003100010061-0

List of Illustrations

Table of Symbols

$F(x)$	Intensity Distribution in Object Space
x	Object Coordinate
$F(\omega)$	Amplitude distribution in frequency space
k	Linear frequency
ω	Radian frequency (2π k) coordinate
$G(\omega)$	Filter characteristic in frequency space
ω_1	Filter cutoff frequency
$H(z)$	Amplitude distribution in image space
z	Image coordinate
T_2	Maximum Transmission level
T_1	Minimum transmission level
c	Variance of the Gaussian pulse

A STUDY OF SPATIAL FILTERING USING THE IMAGE ENHANCEMENT VIEWER

Introduction

The work under the present phase of the contract consisted of two main parts. The first was the modification of the Image Enhancement Viewer and the testing and calibration of this instrument. The second was the continuance of research, in certain areas, which had been carried out by [redacted] while working under previous contracts for the Viewer. STAT

A description of the modified Viewer, along with the methods of testing and calibration is contained in the Operating Manual. Suffice it to say here that the Viewer was put in working order to the specifications listed in the manual.

The following areas of research were investigated:

A non-sharp, Gaussian pluse was theoretically passed through an optical coherent system; its low frequencies were filtered with a high-pass occluding filter, and the final images were plotted.

A filmed non-sharp edge was experimentally filtered using the Viewer, and its image was traced with a scanning photometer. The results were curve fitted, normalized and plotted.

Techniques (in this study, mainly exposure addition) for increasing edge contrast and sharpness using the Viewer were experimentally examined.

The application of various filtering techniques using actual aerial photographs was studied.

Finally, the use of occluding spatial filtering as a tool in the area of photographic mensuration was investigated.

From the study of these five areas, a comprehensive view of the capabilities and limitations of the Image Enhancement Viewer and occluding spatial filtering may be obtained.

Approved For Release 2003/08/04 : CIA-RDP78B04747A003100010061-0

Theoretical Study of the Effect of Occluding Filters on an Unsharp (Gaussian) Pulse

A full description of the Image Enhancement Viewer (Fig. 1) and its basic properties may be found in both the Operation Manual and the [redacted] STAT

STAT [redacted] In operation it employs coherent illumination permitting a treatment that is linear in amplitude.

Since all object films used in the system are immersed in an index-matching fluid (See Manual) there should be no shift in phase, and the object maybe considered solely in terms of amplitude.

In order to obtain a general idea of the effect of occluding filtering on amplitude objects, a generalized case (considered Gaussian for mathematical simplicity) was considered theoretically. This pulse is transformed into the frequency plane and there filtered by a circular, centered occluding filter of generalized dimension. The resulting distribution is then again transformed into a filtered image, which has been computed and plotted for the range at representative values.

Considering a non-sharp pulse of Gaussian form (Fig. 2)

$$f_1(x) = T_2 - \left(T_2 - T_1\right) e^{-cx^2}$$

where $f_1(x)$ is the intensity distribution of a dark centered pulse in the object plane. Its amplitude spectrum in the frequency plane is given by

$$F(\omega) = \int_{-\infty}^{\infty} \left[f_1(x)\right]^{1/2} e^{-i\omega x} dx$$

$\left[f_1(x)\right]^{1/2}$ may then be rewritten in the following form

$$\left[f_1(x)\right]^{1/2} = \left[T_2 - \left(T_2 - T_1\right)e^{-cx^2}\right]^{1/2} = \sqrt{T_2}\left[1 - \left(1 - \frac{T_1}{T_2}\right) e^{-cx^2}\right]^{1/2}$$

Expanding, we get

$$\left[1 - \left(1 - \frac{T_1}{T_2}\right) e^{-cx^2}\right]^{1/2} = 1 - \frac{1}{2}\left(1 - \frac{T_1}{T_2}\right) e^{-cx^2} - \frac{1}{2.4}\left(1 - \frac{T_1}{T_2}\right)^2 e^{-2cx^2}$$

$$- \frac{1.3}{2.4.6}\left(1 - \frac{T_1}{T_2}\right)^3 e^{-3x^2} - \frac{1.3.5}{2.4.6.8}\left(1 - \frac{T_1}{T_2}\right) e^{-4cx^2}$$

$$- \frac{1.3.5.7}{2.4.6.8.10}\left(1 - \frac{T_1}{T_2}\right)^5 e^{-5cx^2} - \ldots\ldots$$

Letting the binomial coefficients be

$$A(1) = \frac{1}{2} \qquad A(4) = \frac{1.3.5}{2.4.6.8}$$

$$A(2) = \frac{1}{2.4} \qquad A(5) = \frac{1.3.5.7}{2.4.6.8.10}$$

$$A(3) = \frac{1.3}{2.4.6}$$

Then $\left[1 - \left(1 - \frac{T_1}{T_2}\right) e^{-cx^2}\right]^{1/2} = 1 - \sum_{n=1} A(n)\left(1 - \frac{T_1}{T_2}\right)^n e^{-ncx^2}$

Putting this in the integral

$$F(\omega) = \int_{-\infty}^{\infty} \sqrt{T_2}\left[1 - \sum_{n=1} A(n)\left(1 - \frac{T_1}{T_2}\right)^n e^{-ncx^2}\right] e^{-i\omega x}\, dx$$

Using the cosine transform, because of symmetry, and the aperture limits

$$F(\omega) = 2\,T_2 \int_0^{x_f} \cos \omega x \, dx - 2\,T_2 \sum_{n=1} A(n) \left(1 - \frac{T_2}{T_1}\right)^n \int_0^{\infty} e^{-ncx^2} \cos \omega x \, dx$$

Integrating

$$F(\omega) = 2\sqrt{T_2}\, xf\, \mathrm{sinc}\left(\omega x_f\right) - \sqrt{T_2} \sum_{n=1} A(n) \left(1 - \frac{T_1}{T_2}\right)^n \frac{\sqrt{\pi}}{\sqrt{nc}}\, e^{-\frac{\omega^2}{4nc}}$$

This pulse may also have a light center in the form

$$f_2(x) = T_1 + \left(T_2 - T_1\right) e^{-cx^2}$$

The expansion and analysis using this pulse is very similar to that of $f_1(x)$.

We then obtain the image of $f_1(x)$, after passing it through a symmetric sharp cutoff occluding filter (Fig. 3)(centered in the frequency plane) whose characteristic is

$$G(\omega) = 1 \qquad \omega_1 \leq \omega \leq \infty$$

$$= 0 \qquad 0 < \omega < \omega_1$$

The distribution in the image plane is given by the following transform

$$h_1(z) = \frac{1}{2\pi} \int_{-\infty}^{\infty} F(\omega)\, G(\omega)\, e^{i\omega x}\, d\omega$$

Again, for reasons of symmetry, we may use the cosine transform

$$h_1(z) = \frac{1}{\pi} \int_{\omega_1}^{\infty} F(\omega) \cos(\omega z)\, d\omega$$

$$= \frac{2\sqrt{T_2}}{\pi} x_f \int_{\omega_1}^{\infty} \operatorname{sinc}(\omega x_f) \cos(\omega z)\, d\omega$$

$$- \frac{\sqrt{T_2}\sqrt{\pi}}{\pi} \int_{\omega_1}^{\infty} \sum_{n=1} A(n) \left(1 - \frac{T_2}{T_1}\right)^n \frac{e^{-\frac{\omega^2}{4nc}}}{\sqrt{nc}} \cos(\omega z)\, d\omega$$

$$= \frac{2\sqrt{T_2}}{\pi} xf \int_{o}^{\infty} \operatorname{sinc}(\omega x_f) \cos(\omega z)\, d\omega - \frac{2\sqrt{T_2}}{T_2} x_f \int_{o}^{\omega_1} \operatorname{sinc}\, \omega x_f \cos(\omega z)\, d\omega$$

$$- \frac{\sqrt{T_2}}{\sqrt{\pi}} \sum_{n=1} A(n) \left(1 - \frac{T_1}{T_2}\right)^n \frac{1}{\sqrt{nc}} \left[\int_{o}^{\infty} e^{-\frac{\omega^2}{4nc}} \cos(\omega z)\, d\omega - \int_{o}^{\omega_1} e^{-\frac{\omega^2}{4nc}} \cos(\omega z)\, d\omega \right]$$

Applying the Trigonometric identity

$$\sin(\omega x_f) \cos(\omega z) = \frac{1}{2} \sin(x_f + z)\, \omega + \sin(x_f - z)\, \omega$$

and integrating, we get

$$h_1(z) = \frac{\sqrt{T_2}}{\pi} \left[\frac{\pi}{2} + \frac{\pi}{2}\right] = \frac{\sqrt{T_2}}{\pi} \operatorname{Si}(x_f + z)\, \omega_1 - \frac{T_2}{\pi} \operatorname{Si}(x_f - z)\, \omega_1$$

$$- \frac{\sqrt{T_2}}{\sqrt{\pi}} \sum_{n=1} A(n) \left(1 - \frac{T_1}{T_2}\right)^n \frac{1}{\sqrt{nc}} \sqrt{n\pi c}\; e^{-cnz^2}$$

$$+\frac{\sqrt{T_2}}{\sqrt{\pi}} \sum_{n=1} A(n) \left(1 - \frac{T_1}{T_2}\right)^m \frac{1}{\sqrt{nc}} \int_0^{\omega_1} e^{-\frac{\omega^2}{4nc}} \cos(\omega z)\, d\omega$$

Finally, the pulse image is given by

$$h_1(z) = \sqrt{T_2} - \frac{\sqrt{T_2}}{\pi} \left[Si\left(x_f + z\right) \omega_1 + Si\left(x_f - z\right) \omega_1\right]$$

$$-\sqrt{T_2} \sum_{n=1} A_n \left(1 - \frac{T_1}{T_2}\right)^n e^{-cnz^2}$$

$$+\frac{\sqrt{T_2}}{\sqrt{\pi}} \sum_{n=1} A(n) \left(1 - \frac{T_1}{T_2}\right)^n \frac{1}{\sqrt{nc}} \int_0^{\omega_1} e^{-\frac{\omega^2}{4nc}} \cos(\omega z)\, d\omega$$

Rewriting the image term in the following from where

$$a = \frac{\omega_1}{\sqrt{2c}}, \qquad m = z\sqrt{2c}, \qquad \frac{\omega}{\omega_1} = t, \text{ and} \qquad d\omega = \omega_1\, dt$$

$$h_1(a,m) = \sqrt{T_2} - \frac{\sqrt{T_2}}{\pi} \left[Si\left(x_f\sqrt{2c} + m\right) a + Si\left(x_f\sqrt{2c} - m\right) a\right]$$

$$- \sqrt{T_2} \sum_{n=1} A(n) \left(1 - \frac{T_2}{T_1}\right)^n e^{-\frac{nm^2}{2}}$$

$$+\frac{\sqrt{T_1}}{\sqrt{\pi}} \sum_{n=1} A(n) \left(1 - \frac{T_1}{T_2}\right)^n \frac{a}{\sqrt{2n}} \int_{-1}^{1} e^{-\frac{a^2t^2}{2n}} \cos(amt)\, dt$$

Since c, the pulse variance is large, than $x_f\sqrt{2c}$ is large and the value of $Si\left(x_f\sqrt{2c} \pm m\right)a$ approaches $\pi/2$. Under this condition, the image reduces to

$$h_1(a,m) = -\sqrt{T_2} \sum_{n=1} A(n) \left(1 - \frac{T_1}{T_2}\right) e^{-\frac{nm^2}{2}}$$

$$+\frac{\sqrt{T_2}}{\sqrt{\pi}} \sum_{n=1} A_n \left(1 - \frac{T_1}{T_2}\right)^n \frac{a}{\sqrt{2n}} \int_{-1}^{1} e^{-\frac{a^2 t^2}{2n}} \cos(amt)\, dt$$

At this point, it is necessary to compute the values of the integral

$$\frac{a}{\sqrt{2\pi n}} \int_{-1}^{1} e^{-\frac{a^2 t^2}{2n}} \cos(amt)\, dt$$

Upon receiving these values, it is then possible to normalize the total energy of the filtered cases to the unfiltered case.

The cases computed were those where "a" had the values of 1/4, 1/2, 1 and 2 and n varied from 1 to 5. m was taken in steps of .05 from 0 to 3.0. T_1 was taken in steps of .01 from 0 to .99. T_2 was set at 1.0.

The normalization procedure is the following

$$\int_{-\infty}^{\infty} \frac{h^2(a, m)}{T_2} = I(a, m)$$

which is normalized to the total energy of the unfiltered pulse $A_p = I(0,m)$ where a = 0. Therefore, the normalization factor is

$$N = \frac{A_p}{I(a,m)}$$

The area of the filtered image, I(a,m) is approximated by Simpson's rule for normalization purposes.

Representative results of the computations were plotted (Fig. 4 a through h).

The parameters relating "k", the linear frequency, and "c", the pulse variance for "a's" varying from 0 to 2 are plotted in Fig. 5. This relationship is defined by

$$c = \frac{2\pi^2 k^2}{a^2}$$

For the entire range of edge contrast (Variation of T_1), the smaller filter sizes give the expected results: increased normalized contrast for increased filter size. The larger filter sizes give rather unexpected and varying results for changing contrast. A full explanation for this phenomenon cannot be made without further study.

Experimental Filtering of a Non-Sharp Edge

In order to substantiate the theoretical work, an experiment was designed with conditions approximating the analysis.

Instead of a pulse, a filmed non-sharp edge was used as an object, being placed in the object plane of the Image Enhancement Viewer. Though this pulse had first been assumed to be of Gaussian shape, subsequent traces have revealed a number of "unGaussian" characteristics which could well affect the resulting filtered traces.

Because an edge was used, and not a pulse, the filters placed in the object plane did not have to be circular (the frequency distribution being one dimensional. The occluding filters used were pieces of drill rod whose width was accurately known. These filters were then carefully centered in the frequency (or filter) plane.

Using a scanning photometer whose slit width was minimized to the point where, at maximum photometer sensitivity, using the largest filter, 100% deflection on the recorder (5 mv range) could be reached. The edge was then traced with the photometer placed in the image plane with its slit parallel with the edge. First, the image of the edge with no occluding filter and the images of the edge with filters corresponding to a - 1.5 and a = 2.5 were traced.

The actual traces for the three cases are found in figure 6. (The two filtered cases are expanded by a factor of ten in the intensity scale:

The resulting filtered cases were normalized to the area under the unfiltered curve in the same manner as used in the theoretical traces. The resulting curves are plotted in figure 7. Because the normalized cases are meant to be compared with the theoretical Gaussian, only the part of the edge corresponding to a pulse (center $\frac{1}{\sqrt{2c}}$ distance from the inflection point)is taken.

Because of differences between the experimental edge and the Gaussian pulse taken in Part I, and the limitations in filter size (it was not possible to obtain smaller filters), no conclusion may be drawn from the results, through a general agreement may be found.

Edge Enhancement Through Exposure Addition

The next area to be investigated was that of actually applying filtering techniques in order to "enhance" an edge on a photographic emulsion. This edge may be enhanced in two different ways; increase in contrast and/or increase in slope.

At present, two methods for producing such enhancement using the Image Enhancement Viewer have been considered. The first is called exposure addition. In this method, an unfiltered edge is exposed on an emulsion, after which an occluding filter is placed in the system and without changing the position of either the edge or the film, a second exposure is made on the same frame. The second method is transmission multiplication. Here, two exposures are made on two separate frames; one exposure is unfiltered, the other, filtered to some degree. These two frames are then combined, using some sort of enlarging technique, in various proportions. Obviously, the difficulty in this method is the alignment of the two negatives which is quite critical. This must be done with an accuracy that would entail a great deal of technical ability.

It was possible to do some work in the area of exposure addition, using the test edges from the previous area, but because of time limitation, it was impossible to do any transmission multiplication.

The edge was exposed, using several occluding filters with varying exposure times, mixing the filtered and unfiltered parts. These edges were then microdensitometered on our Intectron instrument. For these traces, an effective 3 micron slit was used. The results of these traces have been recorded in Table #1.

Tables #1 and #2 refers to exposures #1-19. The slopes (Table #1) and edge contrasts (Table #2) are those read, averaged and weighted from several microdensitometer traces, varied for relative slit position with the edge. Included is the sensitometric curve relavent for the longer exposure times. Given also are the exposure times and the maximum densities (upper point through which the slope passes). As can be seen, some of these values are well up on the shoulder of the sensitometric curve (Table #3). All of the exposures were on Pan-X 70mm film. A plot of the measured edge slopes against the ratio of filtered to unfiltered exposure time is plotted in figure 8.

From this data, it may be concluded that, with correct mixtures of filtered and unfiltered exposures, it is possible to equal, or even surpass, slightly, the slope of the original edge.

Application of Spatial Filtering to the Examination of Aerial Photographs

As part of the studies with the Image Enhancement Viewer, it was considered desirable to examine some aerial negatives with various degrees of spatial filtering. The reason for this was that it is sometimes thought that details below the limit of detection can be brought above this threshold by suitable filtering. Also, it is conceivable that recognition of poorly defined objects might be improved by a controlled filtering which caused ringing at the edges.

When the detail to be detected has a well-defined spectrum, or a known pattern, spatial filtering has definite advantages. For example, a sinusoidal frequency of low modulation, recorded photographically, may be invisible against a grainy background, but by use of a spatial filter permitting only that frequency to pass, the grain "noise" is eliminated from the reconstituted image and the sinusoidal pattern may be seen. To be more precise, only those components of the grain frequency spectrum which lie in the passband of the filter remain to obscure the wanted image, and if the grain spectrum is flat this gives a great improvement in signal-to-noise ratio. However, this is an ideal case for the use of filtering, since the signal spectrum is concentrated at one point in the diffraction plane while the noise spectrum is widely distributed across the plane. When the object is more complex, for example, a square wave instead of a sine wave, its spectrum theoretically extends to infinity, and noise cannot be reduced without distorting the signal in some degree. If the significant feature of the object, however, is its repetitive nature and not the shape of the waves, the filtering can be as effective as for the sinusoidal pattern. For aerial scenes in general, little or no improvement can be expected from spatial filtering, because the details, consisting of sharp edged lines

or similar simple non-repetitive shapes, have very complex spectra. Filtering to reduce noise can only be effective if the objects of interest have simple known spectra, for which individual filters can be made in advance.

To test these ideas under a realistic approximation to practical conditions, the following experimentation was carried out, with a set-up which was being used in another program. Simulated aerial photographs were made by photographing a transparency made under controlled tone-reproduction conditions from a large-scale aerial negative. The original negative scale was 1:2000 and the reduction factor, using a 6 inch lens, was 20 to 1, thus the copy negative were at 1:40,000 scale. Uniform fogging light from a beam-splitter was introduced during the copying, to reduce the luminance scale of the transparency to approximately 5 to 1, simulating an aerial scene viewed from a high altitude. Negatives were made on SO 243 emulsion, varying the lens/film transfer function by changing the lens aperture. These lens/film transfer functions are shown in figure 9; for these values of spatial frequency cut-off, granularity is not obtrusive when looking for detail in the negatives. Thus a series of negatives were available in which the quality of definition showed a progressive deterioration of known amount. The intention was to apply various kinds of filtering, and if any improvement could be seen, to equate this to the quality of the next best negative. Thus any effect of the filtering could be approximately evaluated in terms of the definition of conventionally-viewed photographs.

The original 1:40,000 scale negatives, being only 1 cm in diameter, were enlarged X6, the resulting positive transparencies being more convenient for viewing in the spatial-filtering apparatus. (It was known, from work in the other programs referred to above, that the enlarging process introduced no significant loss of quality even for the best negative.)

After repeated trials of filtering, both high-pass & low-pass, it was concluded that no choice of frequency band enabled anything to be seen which could not be seen as well or better in normal viewing by incoherent light. Indeed, due to the disturbing effect of the ringing around small particles of dirt which had not been completely removed from the negatives or filtered from the fluid, the inooherent viewing was always preferred. In a few instances it was felt that the edges of isolated objects such as trucks might have been more clearly defined when using a high=pass filter, but this effect was so small, (if it existed) that a follow-up with more precise experimentation was not justified.

This negative conclusion is in accordance with the theoretical expectations, as discussed earlier in this section.

It should perhaps be stressed that these findings do not imply that coherent light techniques have no value for the detection of previously-known patterns.

Application of Spatial Filtering to Mensuration

The most obvious practical application of the phenomena produced when the techniques of the Image Enhancement Viewer are used on filmed objects is in connection with mensuration. By using the "ringing" effect found in the vicinity of the edge, it is possible that the location of the edge may be determined with a greater degree of accuracy than may be otherwise obtained.

Using the Viewer, an experiment was devised to test the relative "mensurability" of filtered and unfiltered edges employing a particular measuring instrument. The instrument used was the [redacted] Type 422C Comparator. STAT

A sharp edged, opaque, square object was photographed on SO 243 emulsion at f/6 and at f/1000.

The negatives were then enlarged to a 2" by 2" size, so as to be usable in the Viewer. In order to be able to refer to the original object size, a grating of known dimensions was superimposed on one print of the object. This was measured on the comparator, after having been enlarged and photographed on the Viewer, giving the total magnification of the processes.

The objects were then placed into the Viewer and photographed on 70mm Panatomic-X film, first with no occluding filters used and then with several sized different occluding filters. The exposure level for all of the cases was maintained at approximately the same point.

The dimensions of the photographed square used as an object in the Viewer were determined in two separate manners:

1) The known size of the original cutout was multiplied by the magnification factors of the camera and the enlarger.

2) The object was measured directly on the comparator.

The results given by the two different methods matched to within .01mm. in both directions on the square.

The measurement of the objects, which had been passed through the Viewer, consisted of two parts:

1) It was first necessary to measure the f/6 and f/1000 unfiltered cases to find the accuracy to which the actual object size may be determined. (after having been multiplied by a magnification factor for the Viewer determined separately.) It was found that there was very little difference in the ability to estimate the locations of the edges, and therefore, to measure size of the objects, from the f/6 case to the f/1000 case.

2) After the negatives were filtered with several different sized occluding filters, the measurements to determine the original objects size (multiplied by the known magnification factor of the Viewer, again) were repeated on the comparator.

In the f/6 case, a strong ring was placed on the edge in all the filtering conditions, yet because of the limitations of the comparator and of the ability to place the crosshair at any point with any great accuracy, no improvement of measurement precision was found.

In the f/1000 case, even the largest filter produced very little ringing around the edge position, and once again the filtering did not provide any marked improvement in the ability of locating the edge and measuring the object size.

Measurement of the image of the filtered objects directly on the Viewer was not attempted, though it was quite possible that with a more accurate measuring instrument then was used here, and without the further weakening of the ringing through the recording on film, an improved accuracy in the location of many edges may be found.

CHARACTERISTICS OF TRACED ENHANCED EDGES

Table #1

Exposure No.	Filter (IN)	Average Slope	Unfiltered Time	Filtered Time
1	-	4.5	1/2	-
2	-	3.5	1	-
3	.015	3.2	1/2	1
4	.015	2.5	1/2	2
5	.015	3.6	1/2	4
6	.015	4.3	1	1
7	.015	2.8	1	2
8	.015	2.4	1	4
9	.025	2.8	1/2	2
10	.025	4.0	1/2	4
11	.025	4.1	1/2	8
12	.025	2.8	1	4
13	.025	2.9	1	8
14	.041	2.8	1/2	4
15	.041	3.1	1/2	8
16	.041	5.0	1/2	16
17	.041	3.2	1	4
18	.041	2.0	1	8
19	.041	1.9	1	16

Table #2

Exposure #	Min.	Max.	Contrast
1	.60	1.50	.90
2	.95	1.20	.85
3	.85	1.45	.60
4	1.35	1.80	.45
5	1.55	1.90	.35
6	1.15	1.85	.70
7	1.50	2.00	.50
8	1.40	1.90	.50
9	.80	1.55	.75
10	1.20	1.70	.50
11	1.00	1.60	.60
12	1.10	1.80	.70
13	1.35	1.85	.50
14	.85	1.55	.70
15	.75	1.50	.75
16	.90	1.55	.65
17	.95	1.70	.75
18	1.30	1.80	.50
19	1.65	2.25	.60

STAT

TABLE #3

[redacted] CURVES FOR

ENHANCED EDGES

PANATOMIC-X, D-19 6 MIN.

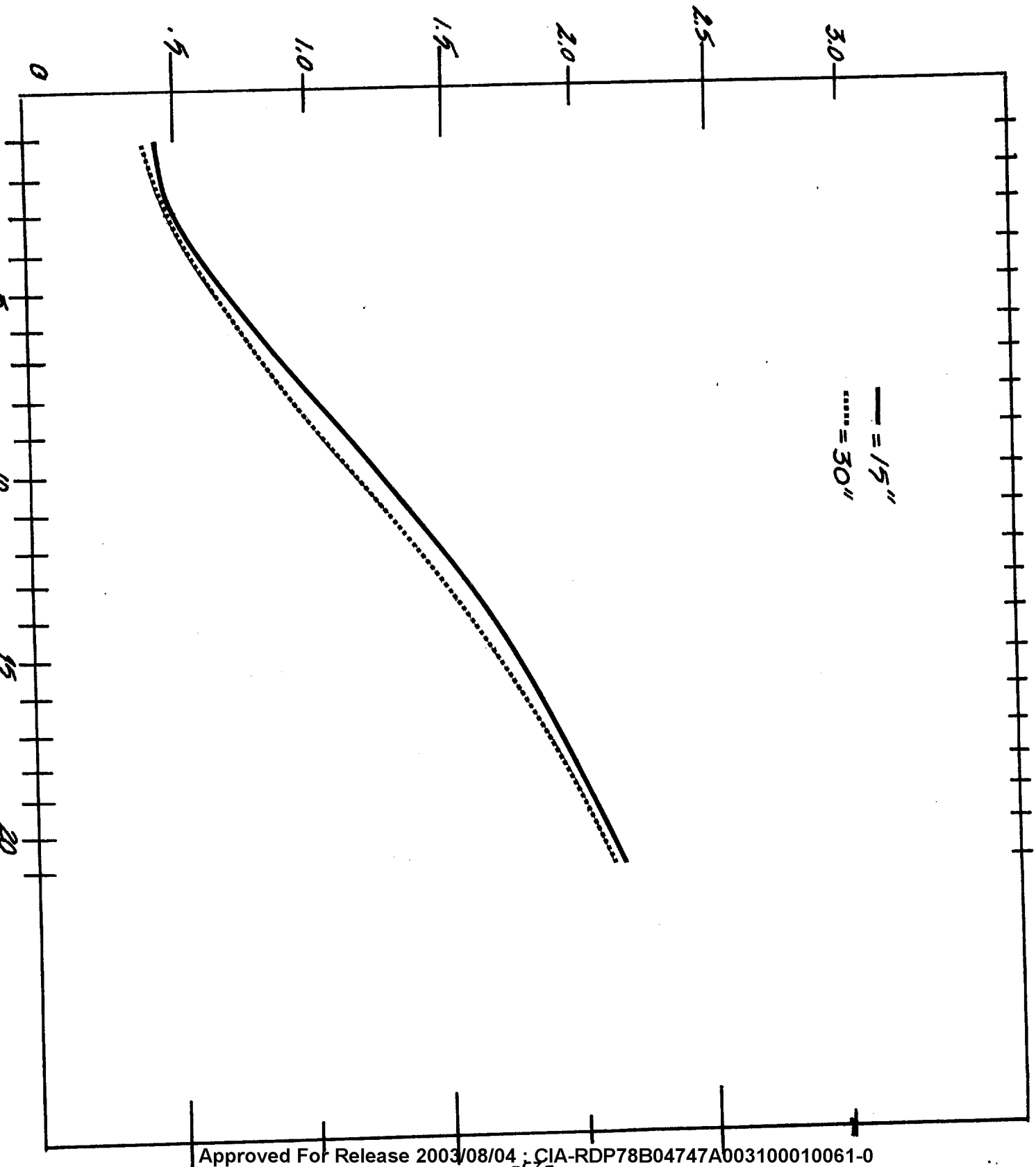

Major Features and Dimensions of Image Enhancement Viewer

(Approximate overall system length = 8 feet)

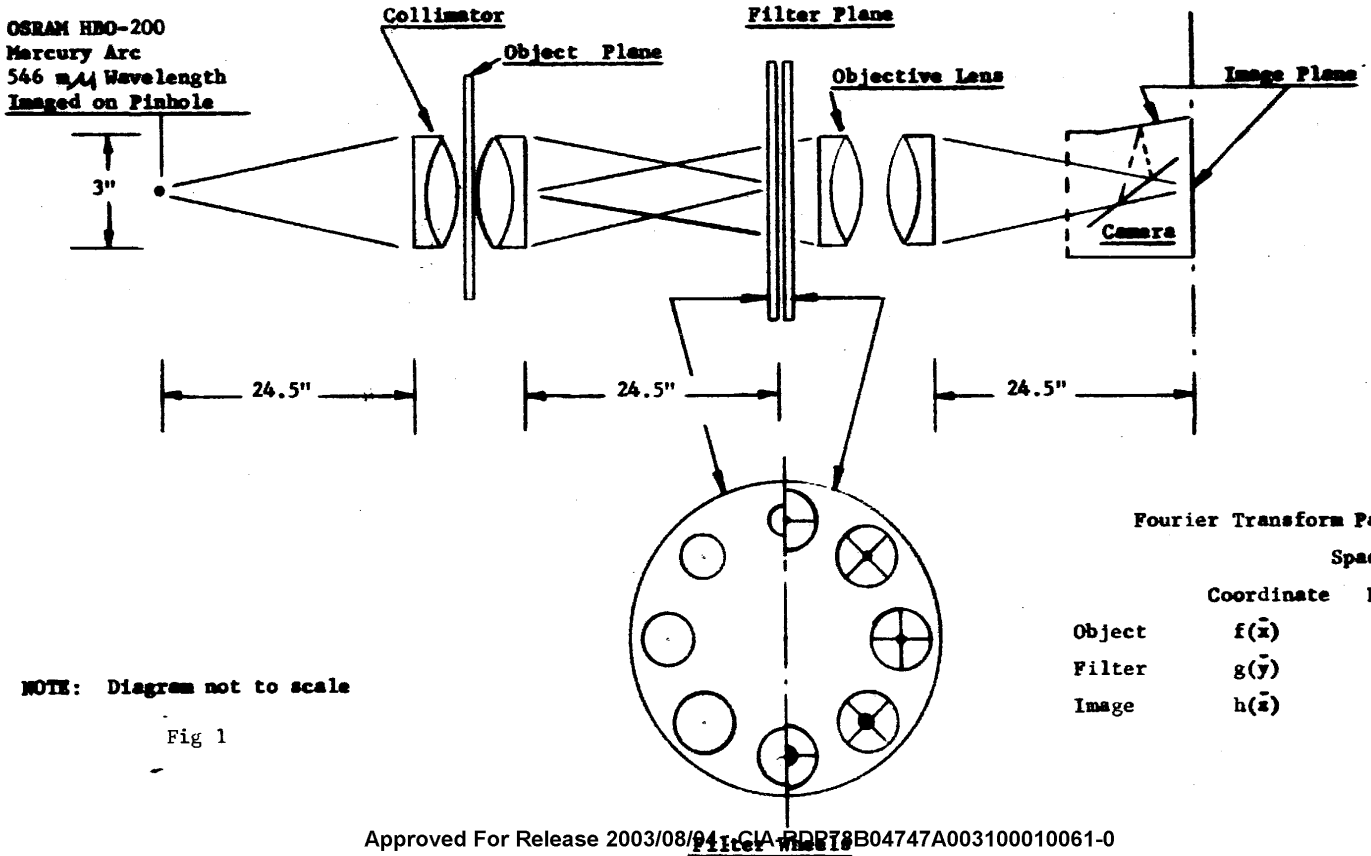

NOTE: Diagram not to scale

Fig 1

Fourier Transform Pairs

	Space Coordinate	Frequency
Object	$f(\bar{x})$	$F(\bar{w})$
Filter	$g(\bar{y})$	$G(\bar{w})$
Image	$h(\bar{z})$	$H(\bar{w})$

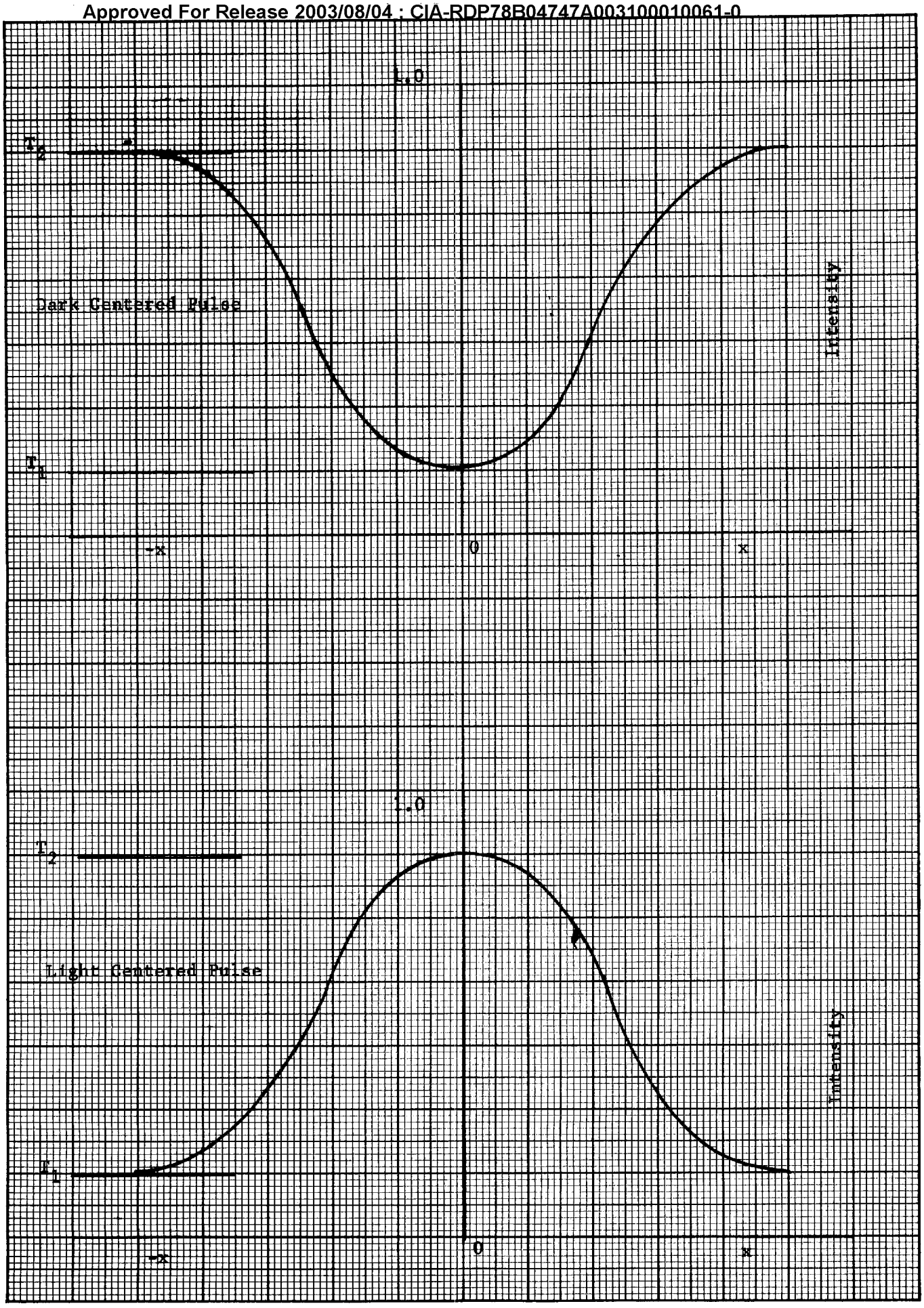

 Fig. 2

GAUSSIAN SPATIAL PULSE WITH OCCLUDING SPATIAL FILTER

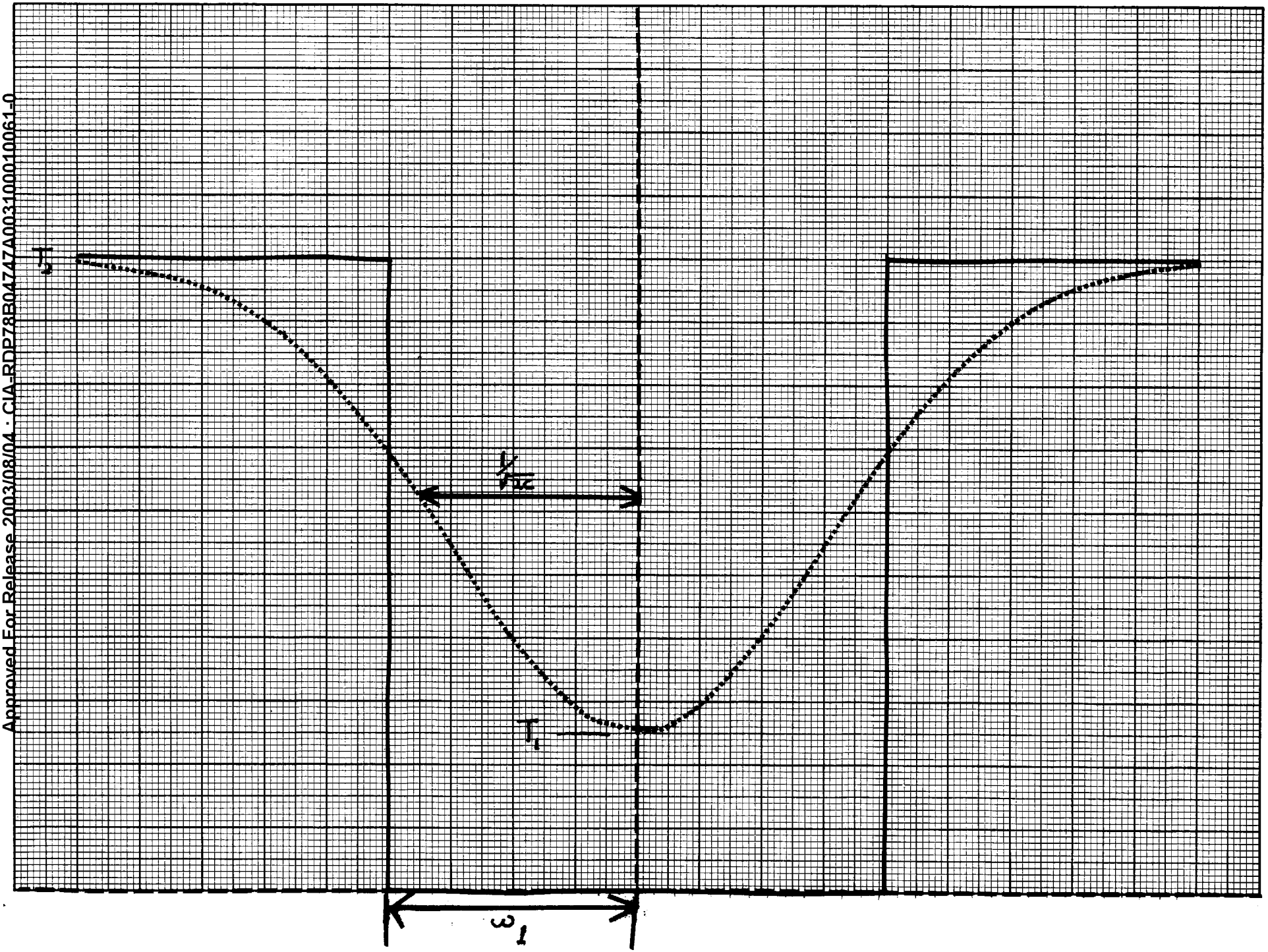

Fig. 3

Approved For Release 2003/08/04 : CIA-RDP78B04747A003100010061-0

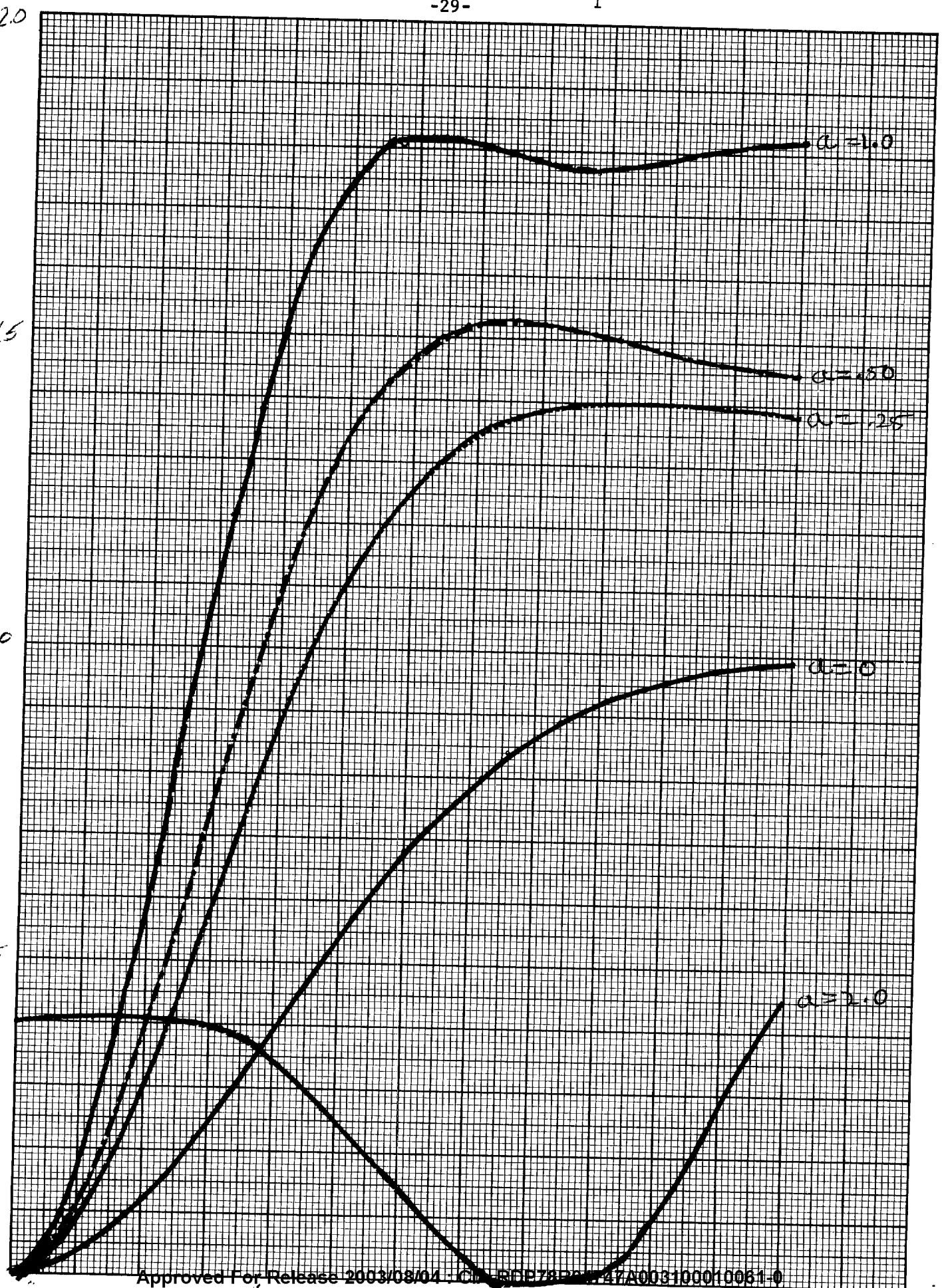

Fig 4a

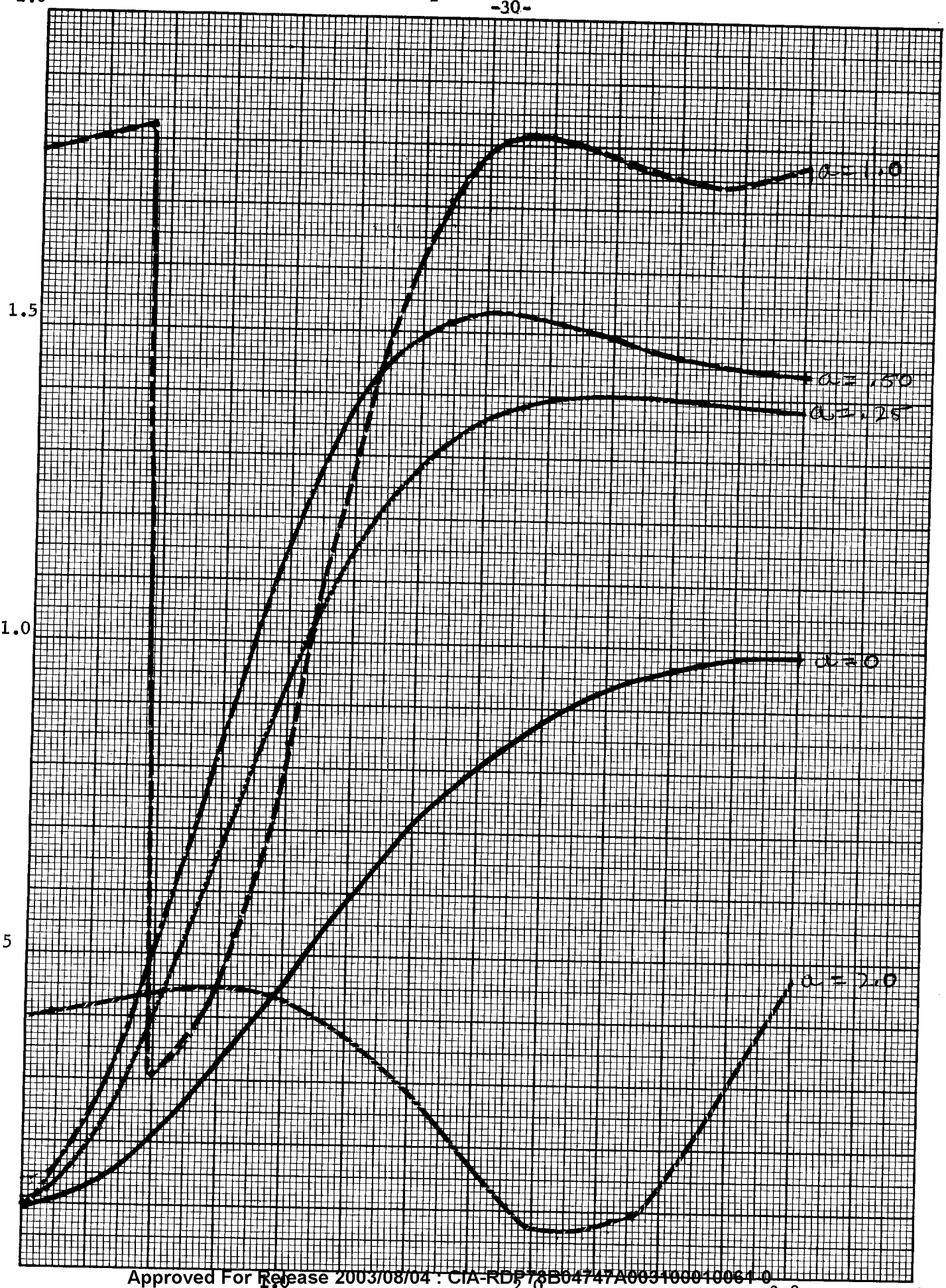

Fig. 4b

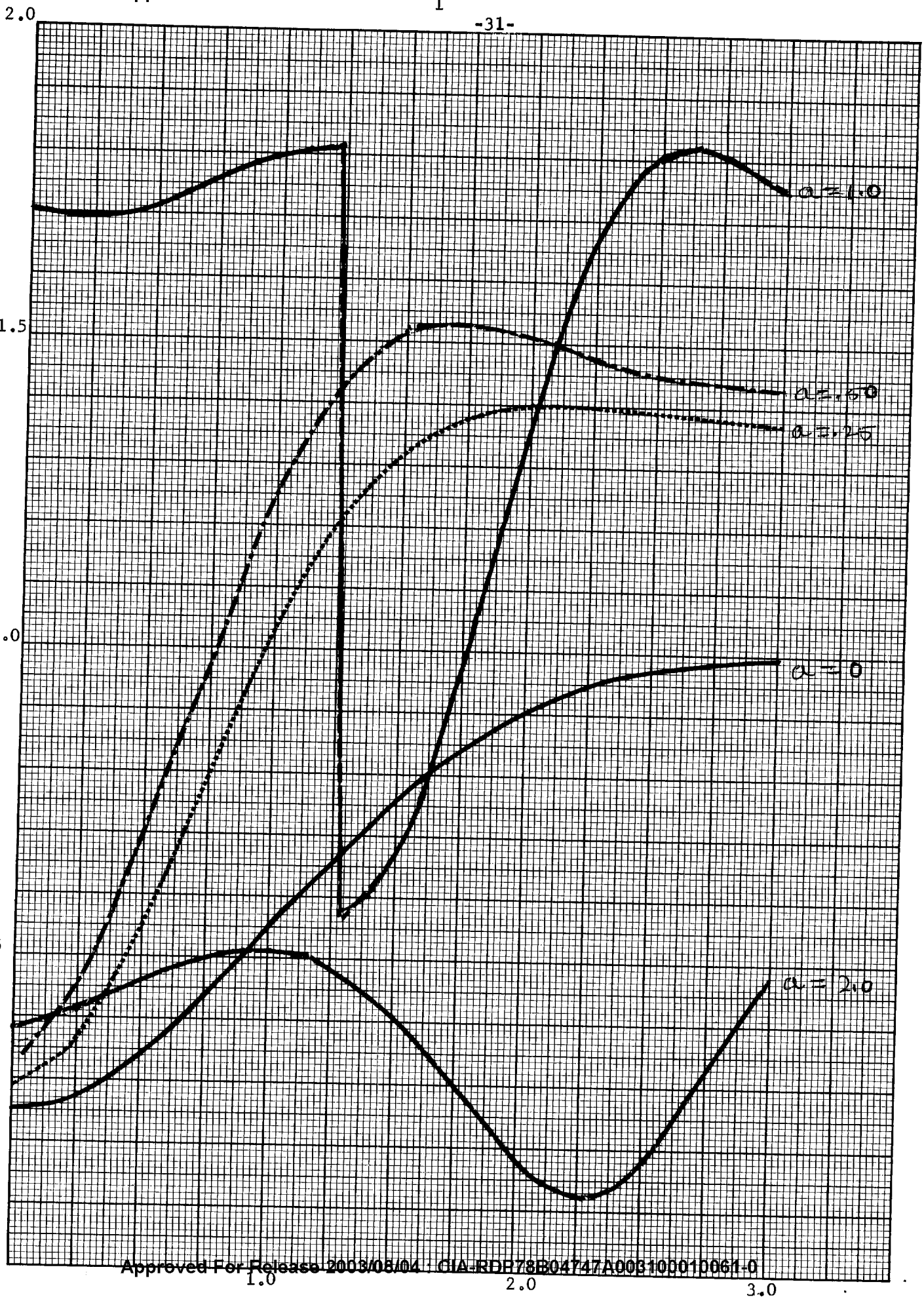

Fig. 4c

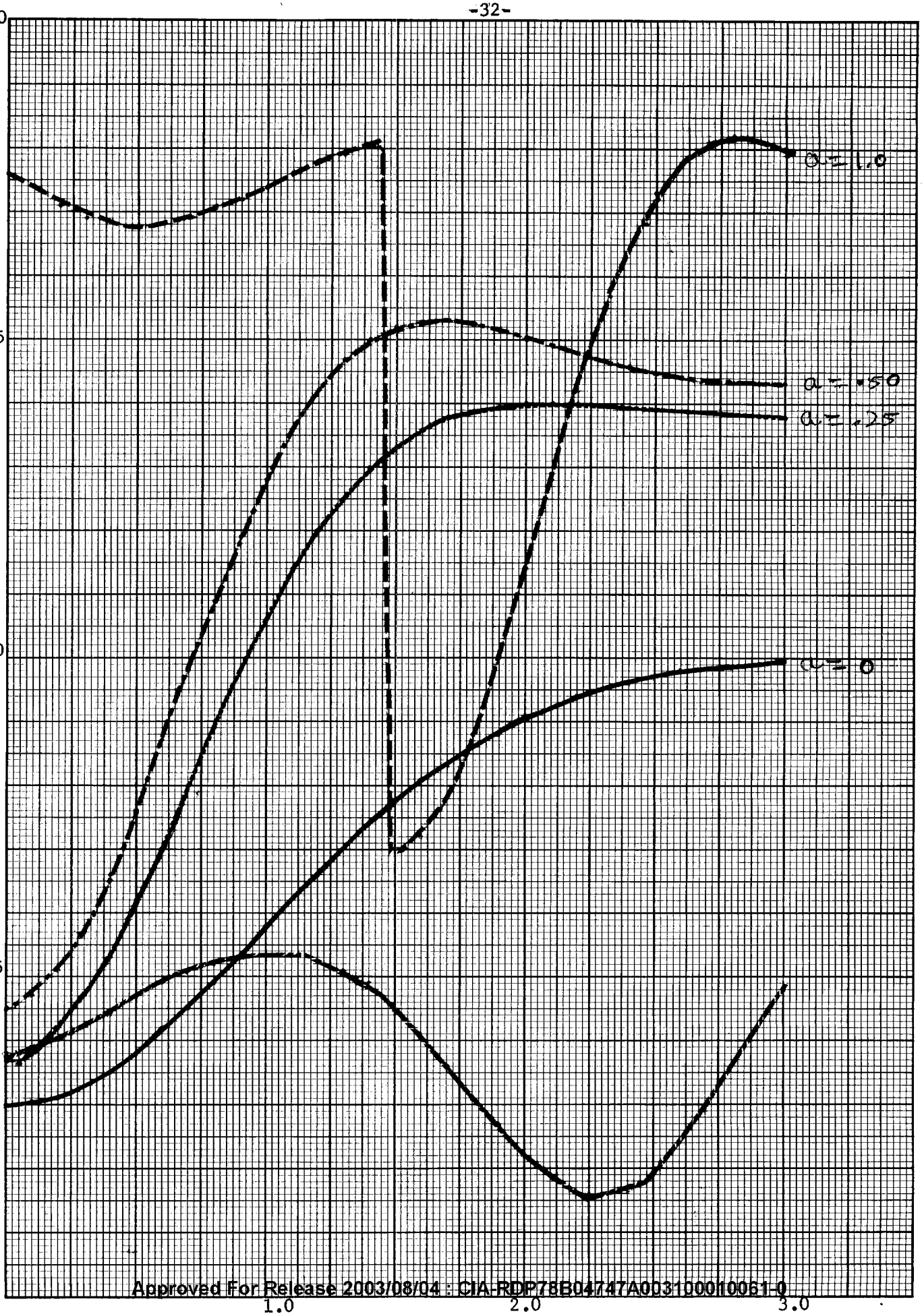

Fig. 4d

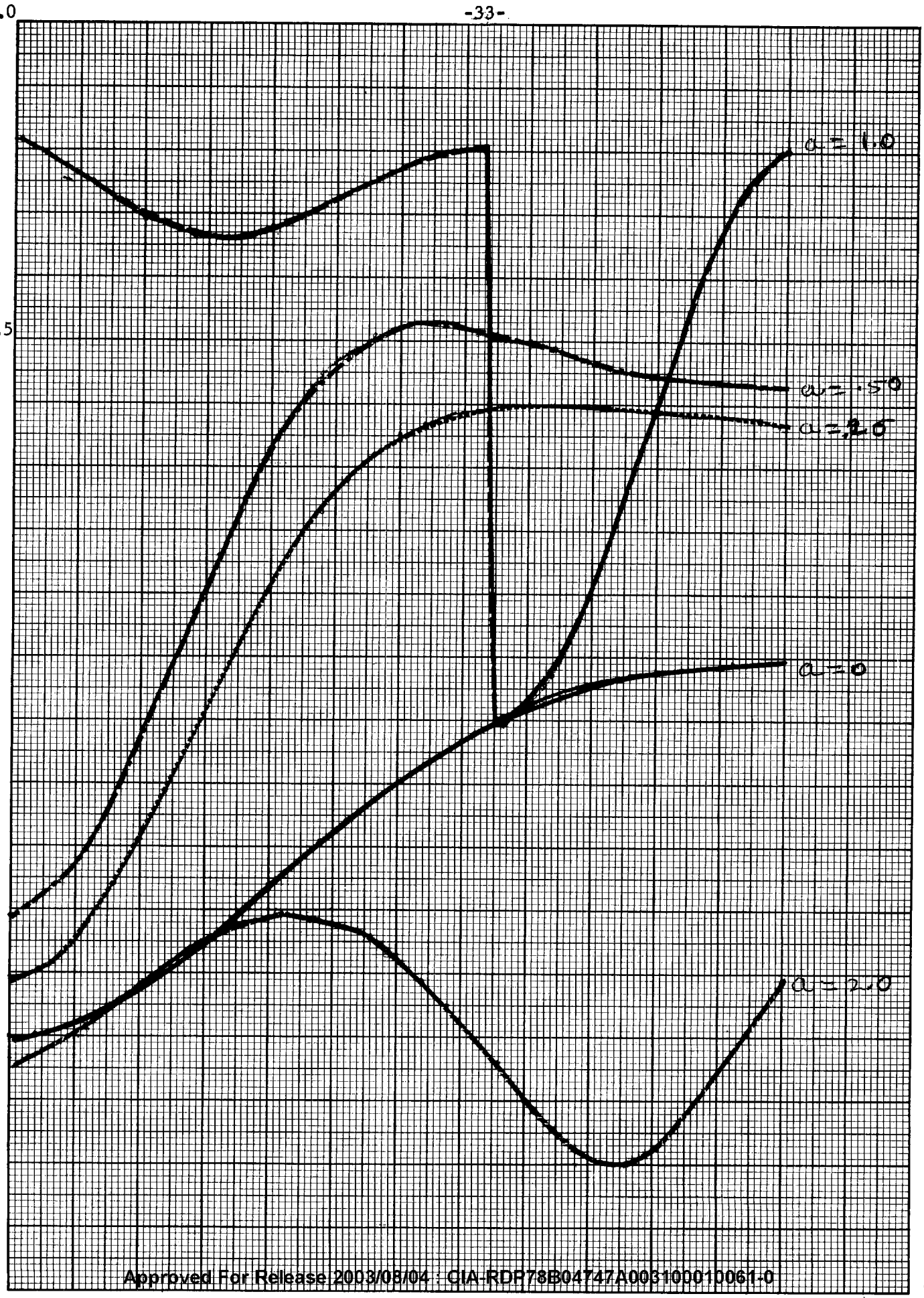

Fig. 4e

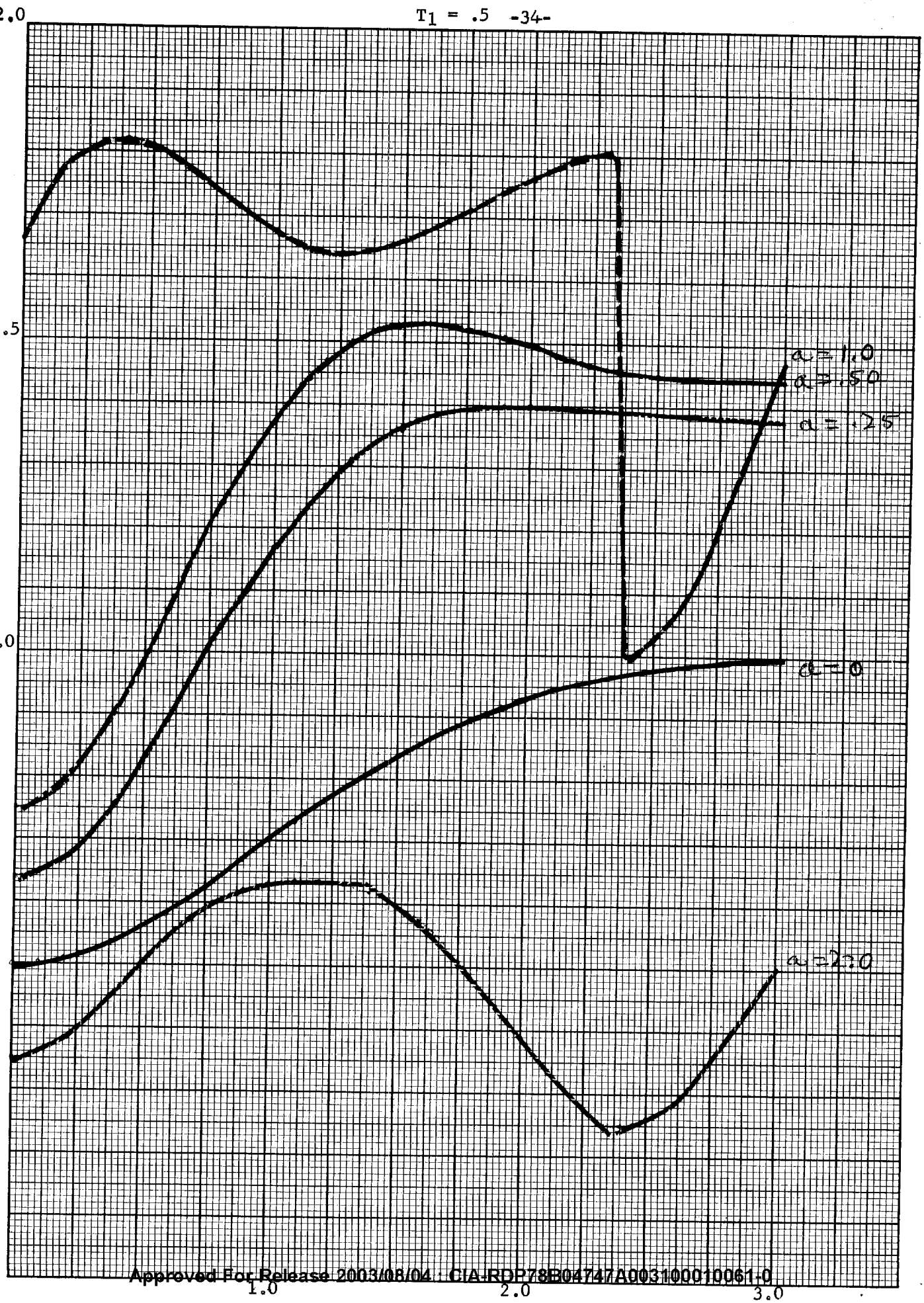

Fig. 4f

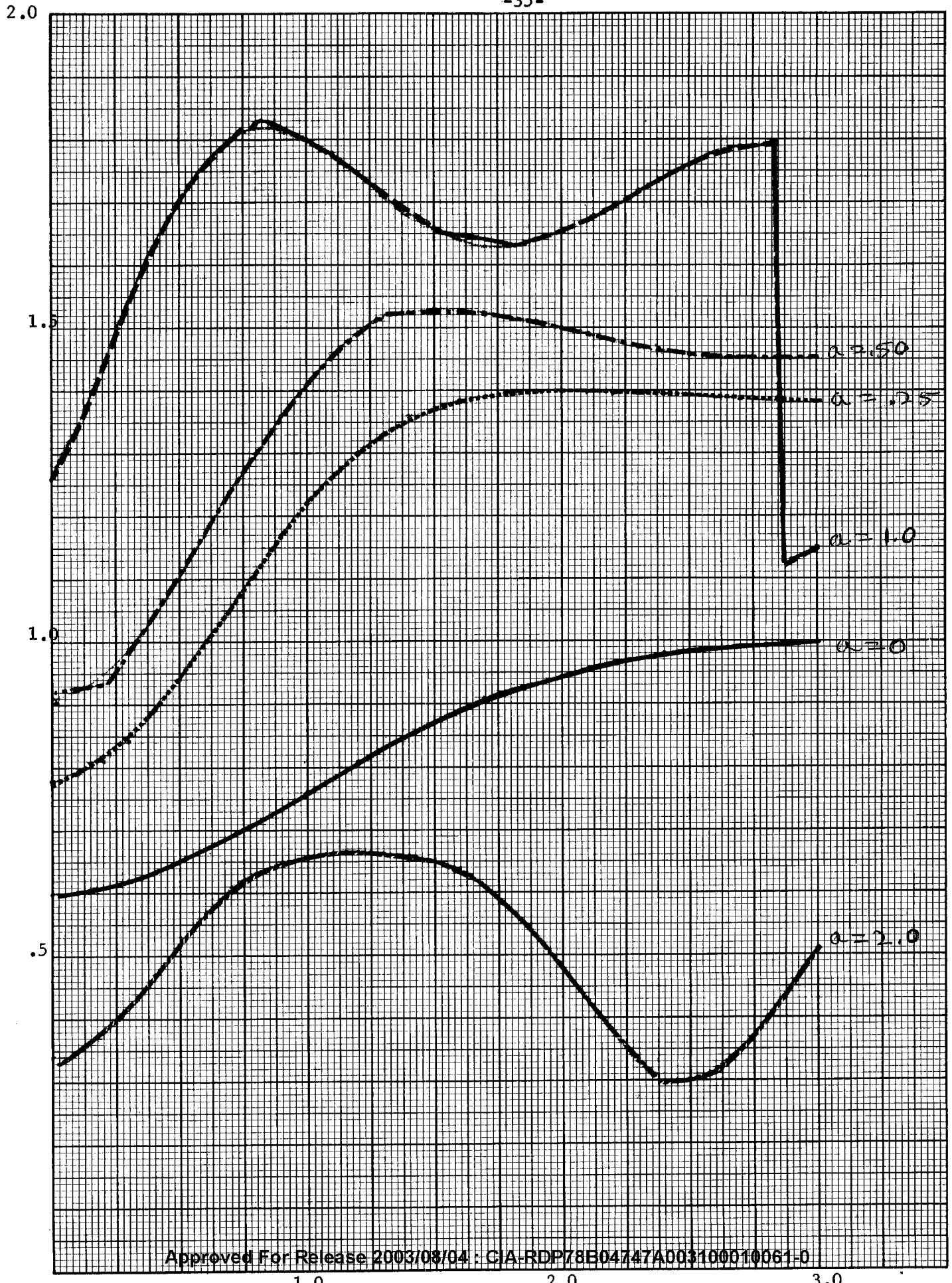

Fig. 4g

$T_1 = .7$

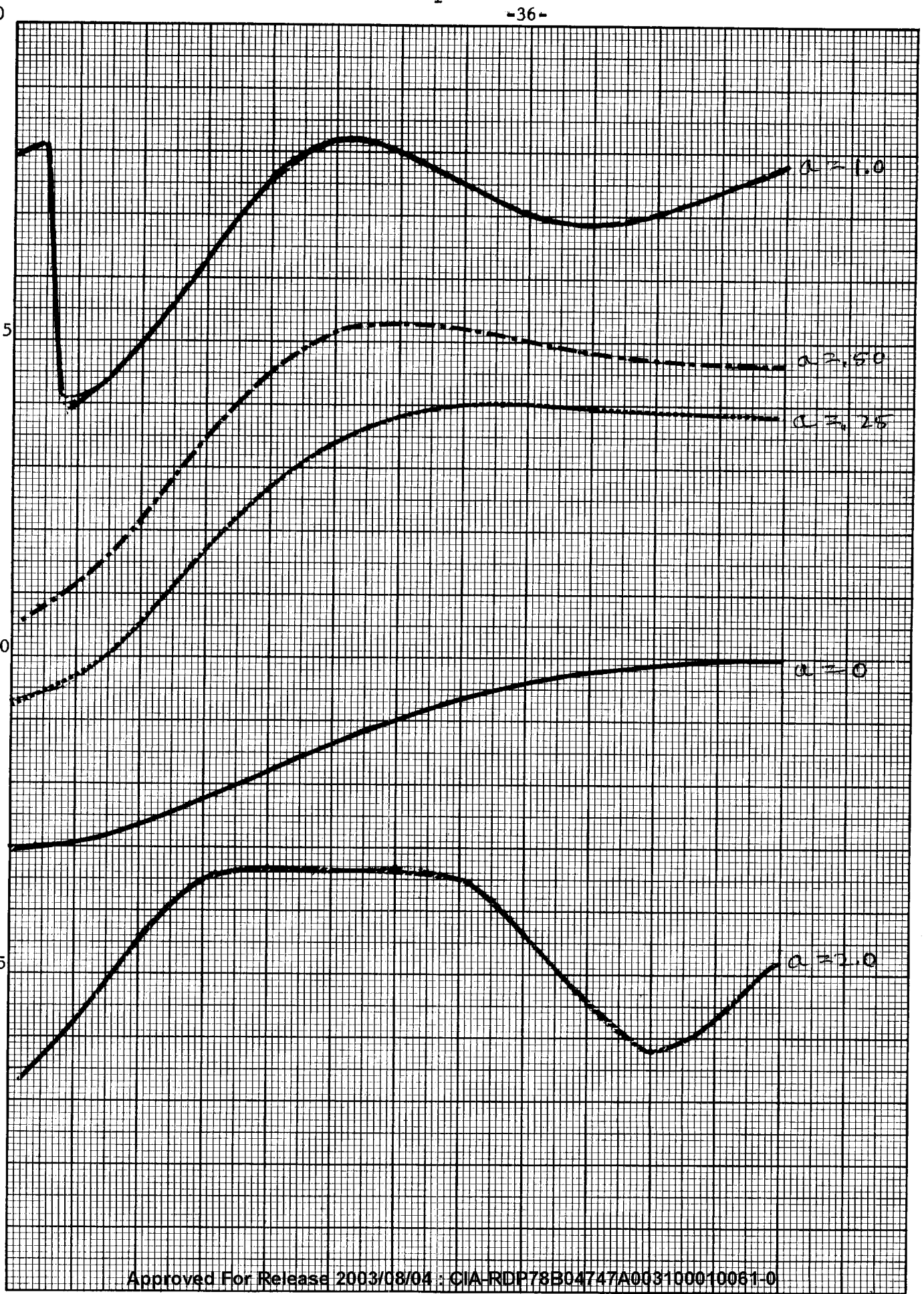

Fig 4h

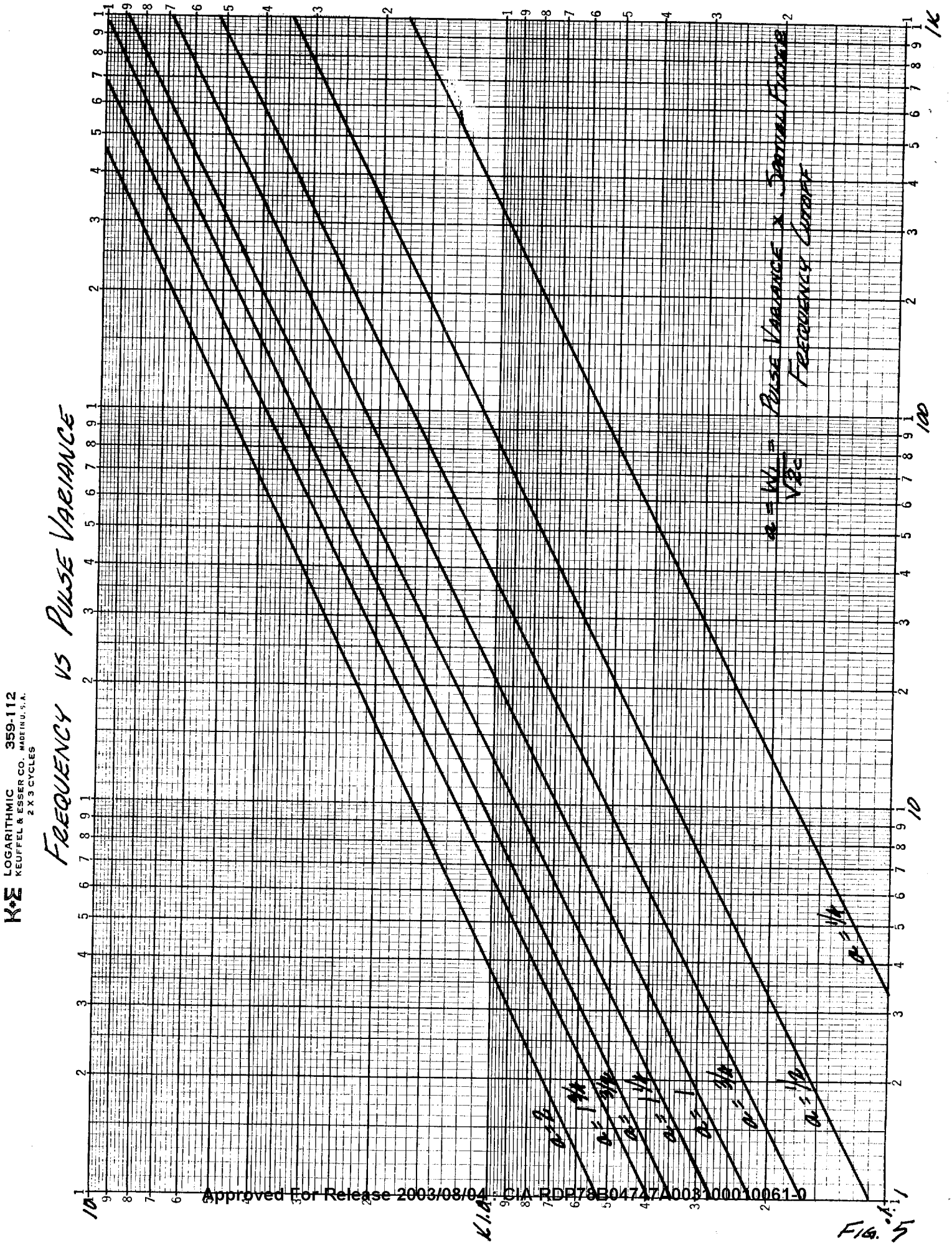

FIG. 5

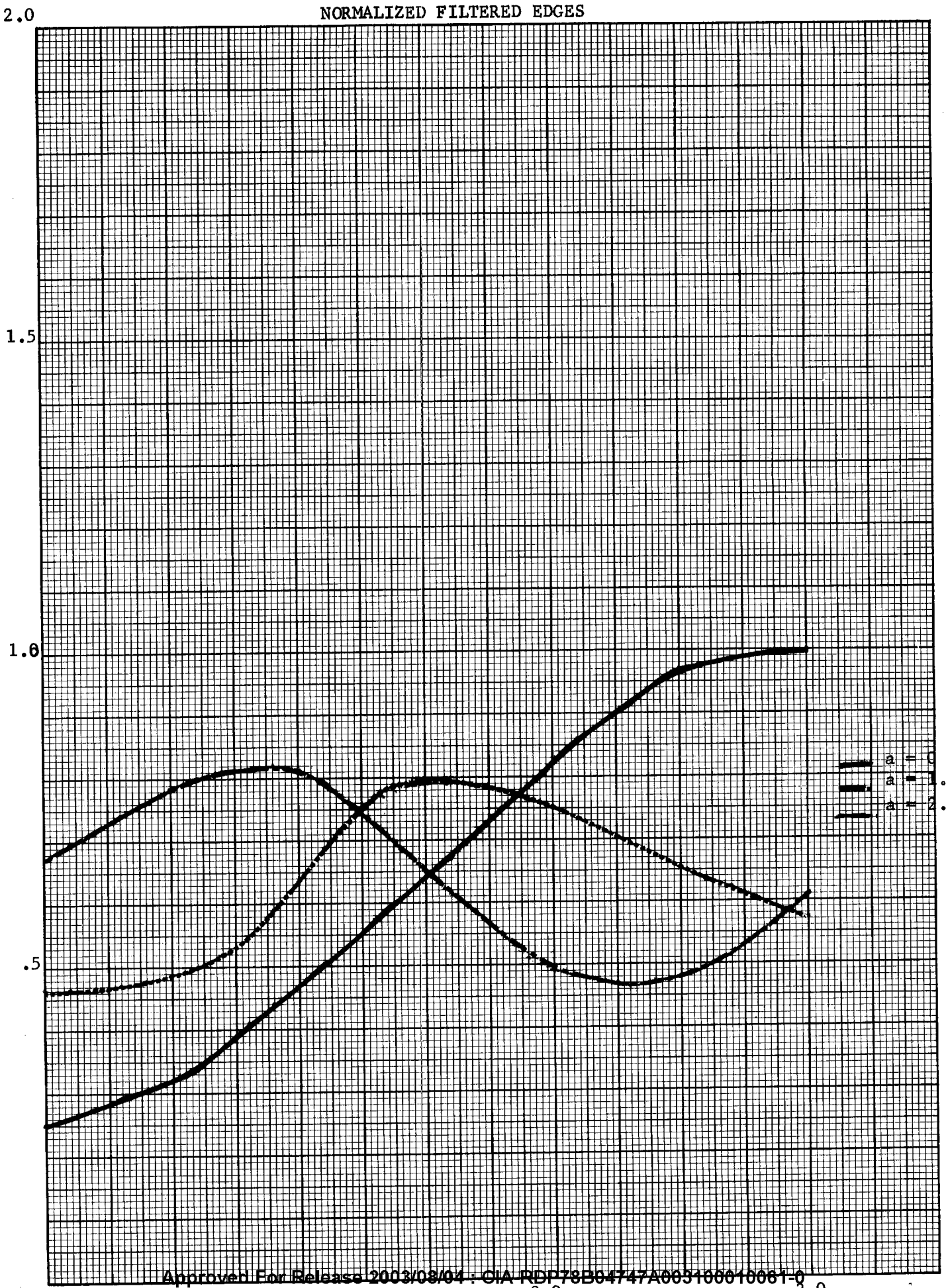

Fig. 7

CHANGE OF EDGE SLOPE WITH VARYING EXPOSURE TIME RATIO
USING EXPOSURE ADDITION

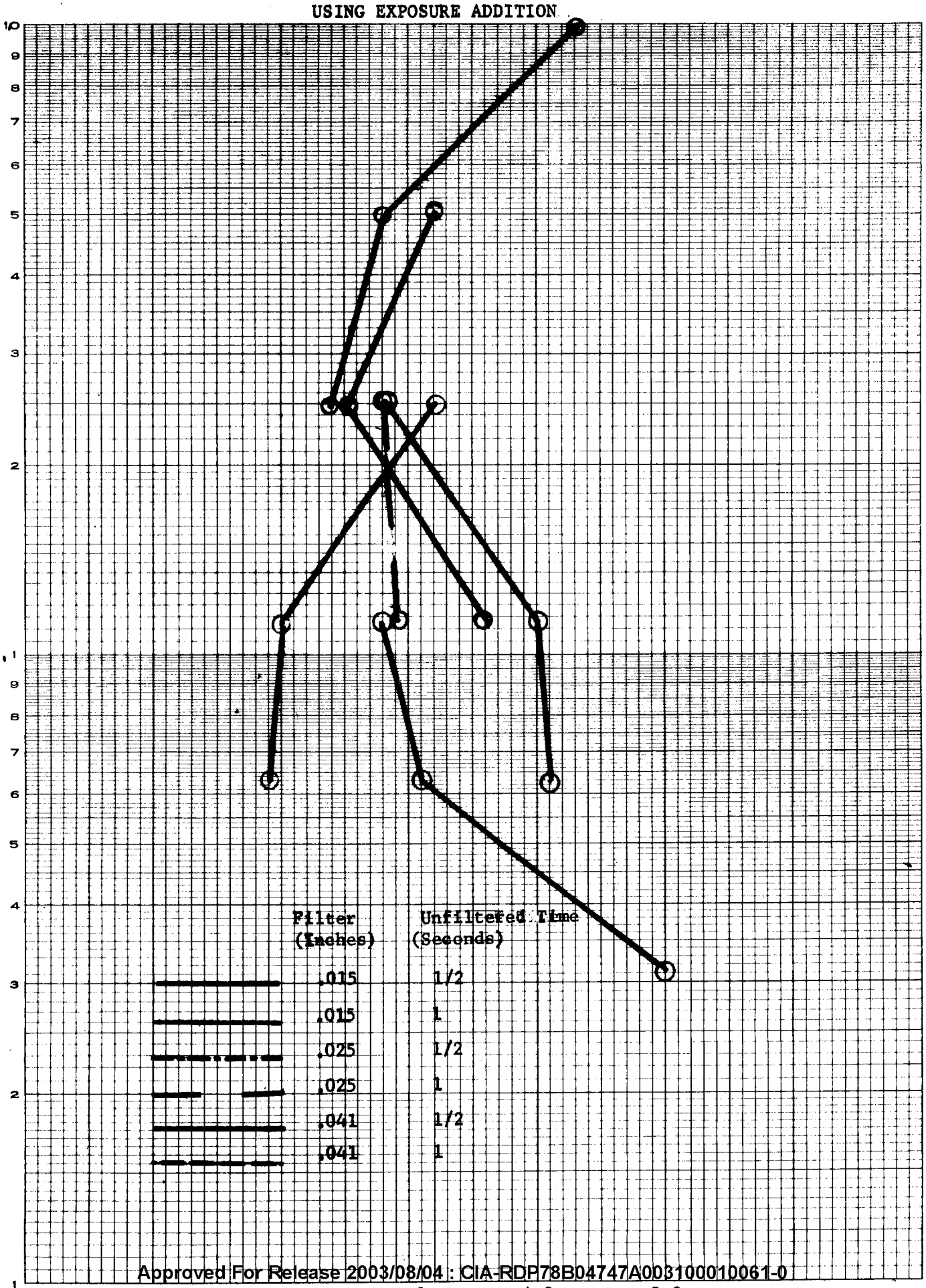

Fig. 8

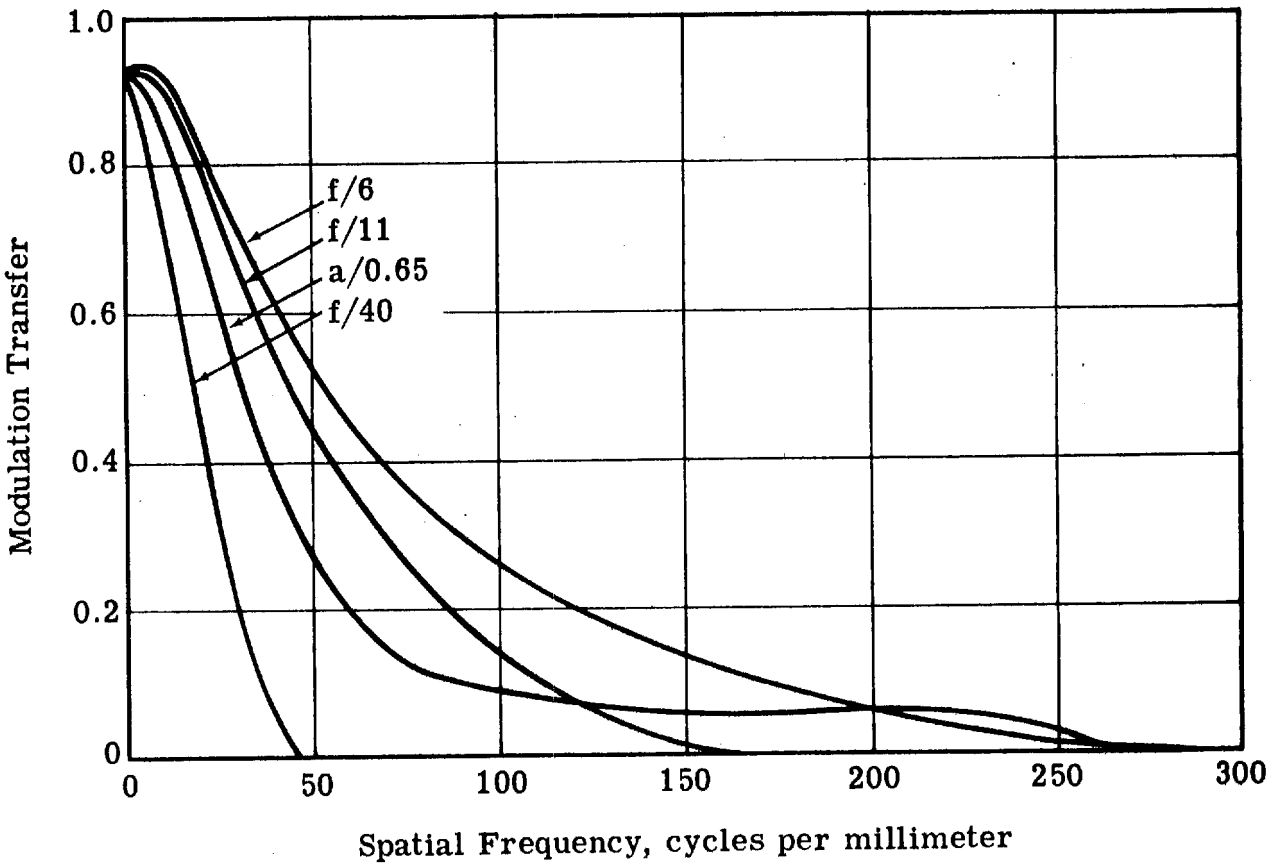

Four lens-film transfer functions: SO-243

Fig. 9

MEMORANDUM FOR: Ed S.

Here is Sepia copy of Mat's final report

Corrected! Buch was apologetic and apoplectic — he chewed friend Peter N. out real nice! pel.

[redacted]

MEMORANDUM FOR:

He still did not take care of Figures 6, 7, 8

(DATE)

FORM NO. 101 REPLACES FORM 10-101 WHICH MAY BE USED.
1 AUG 54 (47)

Approved For Release 2003/08/04 : CIA-RDP78B04747A003100010061-0